Design and Evaluation of a 3-DoF Haptic Device for Directional Shear Cues on the Forearm

Kyle T. Yoshida, Zane A. Zook, *Member, IEEE*, Hojung Choi, *Graduate Student Member, IEEE*, Ming Luo, *Member, IEEE*, Marcia K. O'Malley, *Fellow, IEEE*, and Allison M. Okamura, *Fellow, IEEE*

***Abstract*—Wearable haptic devices on the forearm can relay information from virtual agents, robots, and other humans while leaving the hands free. We introduce and test a new wearable haptic device that uses soft actuators to provide normal and shear force to the skin of the forearm. A rigid housing and gear motor are used to control the direction of the shear force. A 6-axis force/torque sensor, distance sensor, and pressure sensors are integrated to quantify how the soft tactor interacts with the skin. When worn by participants, the device delivered consistent shear forces of up to 0.64 N and normal forces of up to 0.56 N over distances as large as 14.3 mm. To understand cue saliency, we conducted a user study asking participants to identify linear shear directional cues in a 4-direction task and an 8-direction task with different cue speeds, travel distances, and contact patterns. Participants identified cues with longer travel distances best, with an 85.1% accuracy in the 4-direction task, and a 43.5% accuracy in the 8-direction task. Participants had a directional bias, with a preferential response in the axis towards and away from the wrist bone.**

***Index Terms*—Wearable haptics, cutaneous haptic feedback, skin shear, pneumatic actuation.**

I. Introduction

WEARABLE haptic devices can provide feedback during interactions with robots, virtual agents, and other humans. One of the most convenient places for a wearable haptic device is the forearm, due to its accessibility, distance from major joints, proximity to the hand, and social familiarity as a place where watches and bracelets are commonly worn [1]. Haptic devices for the forearm have been used in a variety of scenarios to provide proprioception [2], [3], [4], directional cues [5], [6], force feedback [7], and augmentation in virtual reality environments [8]. Haptic devices for the forearm have advantages over traditional desktop, palm, and fingertip devices because they leave the hands free to interact with other objects or to perform other tasks [9]. This can be especially useful for communicating information without interfering with object manipulation [9].

Although wearable haptic devices on the forearm leave the hands free, they also present perceptual challenges due to differences in mechanoreceptor type and density. Mechanoreceptors primarily targeted by haptic devices include Pacinian Corpuscles for vibration, Merkel Cells for pressure, Meissner Corpuscles for skin deformation and skin slip, Ruffini endings for skin stretch, and C-tactile Afferents for stroking sensations [10], [11]. Notably, the forearm has less than 5% of the mechanoreceptor density of the fingertips [12], making it difficult to provide salient tactile cues. Thus, wearable haptic devices created for the forearm often have large contact areas composed of arrays of actuators [13] or use multiple 1-DoF actuation modes [14] to stimulate different types of mechanoreceptors.

Wearable haptic devices have integrated multiple types of cues including vibration, shear force, and normal force feedback to interface with different mechanoreceptors [15]. Shear forces in particular, have been used to convey directional cues [5], [16] and virtual object properties such as mass, stiffness, and friction in a single contact point [7], [8]. However, incorporating shear can complicate designs for rigid devices that use only servo and gear motors, often necessitating complex gearing and transmission systems. Because of this, wearable haptic devices for shear on the forearm exist primarily as 1-DoF [8], [17] or 2-DoF [5], [16] devices that maintain contact with the skin. For instance, Kuang et al. developed a wearable, 2-DoF device that uses two servo motors to move a metallic sphere across the skin on the forearm [5]. This device provides lateral stretch over a 12×12 mm workspace and can assist with navigation in walking tasks. Kuniyasu et al. created a 2-DoF device that is placed on the top and bottom of the forearm to provide 8–15 mm of shear to provide four directional cues [3]. Caswell et al. conducted perceptual experiments to show that a displacement of 0.5 mm on the forearm yields a four-direction accuracy of 93%, and created a device that can provide 2-DoF shear feedback using two servos [6]. Sarac et al. developed a wearable, 1-DoF device that uses one servo motor to provide shear on the forearm that can stretch over a 20 mm workspace [8].

Manuscript received 22 June 2023; revised 14 December 2023 and 26 January 2024; accepted 30 January 2024. Date of publication 13 February 2024; date of current version 19 September 2024. This work was supported in part by the National Science Foundation under Grant 1830163 and Grant 1830146, in part by the National Science Foundation Graduate Fellowship Program, and in part by the Stanford Graduate Fellowship. This paper was recommended for publication by Associate Editor M. Bianchi and Editor-in-Chief D. Prattichizzo upon evaluation of the reviewers' comments. *(Corresponding author: Kyle T. Yoshida.)*

This work involved human subjects or animals in its research. Approval of all ethical and experimental procedures and protocols was granted by Stanford University Institutional Review Board under Application No. 22514.

Kyle T. Yoshida, Hojung Choi, and Allison M. Okamura are with the Mechanical Engineering Department, Stanford University, Stanford, CA 94305 USA (e-mail: kyle3@stanford.edu; hjchoi92@stanford.edu; aokamura@stanford.edu).

Zane A. Zook and Marcia K. O'Malley are with the Mechanical Engineering Department, Rice University, Houston, TX 77005 USA (e-mail: zzook@alumni.rice.edu; omalleym@rice.edu).

Ming Luo is with the School of Mechanical and Materials Engineering, Washington State University, Pullman, WA 99164 USA (e-mail: ming.luo@wsu.edu).

Digital Object Identifier 10.1109/TOH.2024.3365669

Recently, haptic devices using pneumatics [18] have also emerged due to their ability to produce feedback with lightweight actuators. Raitor et al. developed WRAP, which used pneumatic pouches made from an inextensible thermoplastic to provide directional information using normal force feedback on the wrist [13]. Each pouch had one degree of freedom, so an array was needed to relay directional cues at multiple contact points. Kanjanapas et al. developed a 2-DoF shear display using elastomeric soft actuators that provide salient linear shear cues at a single contact point with travel distances of up to 8 mm with about 1 N of shear force [16]. However, the performance of this device was limited, because the tactor could not make and break contact with the skin.

To increase the saliency of linear shear cues, we previously, developed a 3-DoF haptic device that uses a motor to orient a soft tactor, allowing it to produce shear at any angle, in combination with a new soft actuator system that could make and break contact with the skin [19]. This design consisted of both soft portions (for linear actuation) and rigid portions (for the housing and rotational actuation), and it was able to produce arcs, torsion, vibration (induced by motor oscillations or pneumatic pulsing), shear, and normal indentation.

A key advantage of pneumatic actuation is the ability to provide linear motion through pressure-driven expansion. Thus, a single soft actuator can replace a complex mechanical linear actuation system using multiple motors, lead screws, and gears. These soft, pneumatic actuators easily achieve linear motion and allow us to build lightweight, wearable devices, with off-board air sources for actuation, that can deliver shear force. Tethering to an external air pressure source can also inhibit the overall wearability and mobility of a pneumatic device, but this could be fixed by integrating a wearable pump for a pressure source [20]. For this paper, we were more interested in the device itself, as pneumatic options for tethered and un-tethered options already exist.

While pneumatic actuators provide linear motions quite naturally, they have not been developed to produce large, uncoupled rotational motions. Rotational motions are needed in this design to allow the soft actuators to create shear in multiple directions. Because of this, we created a device that uses a hybrid actuation system consisting of both pneumatic actuators and a traditional gear motor. Soft actuators provide linear motion and form soft contact with the skin, while a motor provides rotation to orient the soft actuators to deliver shear force in a specific direction. Prior work has shown that fully soft wearable devices result in noticeable, undesirable reaction forces [16]. Thus, rather than developing a completely soft device, we also use a rigid housing to prevent noticeable reaction forces and improve cue salience.

In this paper, we further develop a 3-DoF wearable haptic device that uses soft, pneumatic actuators to produce shear cues [19]. We integrate a 6-axis force/torque sensor, a distance sensor, and pressure sensors to record forces, lateral tactor travel distance, and pressure. We show how the device can create different conditions of shear cues that vary based on distance, contact pattern, and contact time. Using four different shear cues, we conducted a user study to determine the relationship between cue condition and participant accuracy and analyze how participant accuracy relates to the physical capabilities of the device, specifically the normal force, shear force, travel distance, and actuator air pressure delivered during each cue. Our study shows the accuracy with which participants perceived linear shear cues from the device and provides insight into the design of future wearable haptic devices.

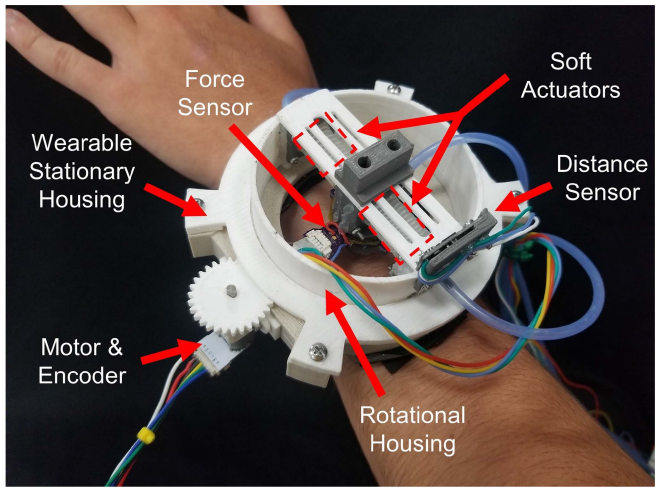

Fig. 1. 3-DoF haptic device on the forearm. The haptic device features soft actuators for linear motion and a rigid DC motor for rotation. The device has a built-in force sensor and a distance sensor to measure tactor forces and motion.

In summary, our experience in designing the previous wearable devices described in Yoshida et al. [19] and Kanjanapas et al. [16] taught us that soft materials do not provide adequate force grounding to the arm. However, soft materials are effective at providing linear motion in haptic devices. We also found that using a rigid housing produced more salient cues due to the grounding of reaction forces. In this paper, we re-design a haptic device for the forearm to include sensing and conduct user studies to understand how participants identify directional cues from the device. The main contributions of this paper are:

- A new device (Fig. 1) based on previous work by Yoshida et al. [19] that adds pressure, distance, and force sensing
- Force and displacement measurements from the device when delivering shear
- Two user studies to understand how participants perceive either 4 or 8 directional shear cues on the forearm
- Analysis showing how travel distance, contact pattern, and cue duration impact participant perception accuracy

II. Device Design

We present a device that builds on work by Yoshida et al. [19], using a hybrid actuation system consisting of soft actuators and a DC motor. The soft actuators in [19] provided linear movement, while the DC motor provided rotation to orient the direction in which the soft actuators can provide shear forces. Here, we update the design of the soft actuators to simplify fabrication. Furthermore, we integrate force, pressure, and distance sensors to calibrate the device for each participant and analyze device performance during use.

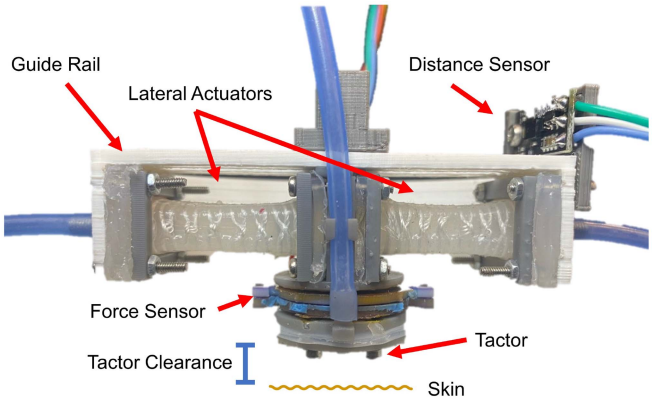

Fig. 2. Cross section of the rotational housing showing the soft actuator assembly. The T-shaped soft actuator assembly is comprised of three pneumatic chambers, two lateral actuators and one tactor. The two lateral actuators are fiber-constrained linear actuators, and the tactor is a silicone sheet that balloons out to control normal indentation. Above the tactor is a thin 6-axis force/torque sensor. At the top of the device is a distance sensor that measures the lateral distance that the tactor travels with respect to its center position. The tactor is constrained by a guide rail such that there is no bending moment. The bottom of the tactor has a clearance of 0.5 cm above the skin when not pressurized and touches the skin when pressurized.

Three soft actuators are used, placed to form a T-shaped assembly (Fig. 2). This is comprised of two lateral actuators and a tactor. The lateral actuators are fiber-reinforced elastomeric enclosures that produce linear elongation when pressurized [21], [22]. These are created by casting silicone (Ecoflex 00-30, Smooth-On) into a 3D-printed, cylindrical mold. After the lateral actuators are cured, a double-helix threaded constraint is applied to the exterior to restrict radial expansion, resulting in only elongation. At the end of each lateral actuator, a soft, square end-cap (DragonSkin 30, Smooth-On) is attached using a silicone adhesive (Sil-Poxy, Smooth-On). This end cap allows for a wider base to attach to the rigid housing of the device. Each end-cap has a hole with a vent-screw inserted to attach tubing to the actuator for air flow. The tactor is created by casting a 3 mm thick sheet of silicone (DragonSkin 10, Smooth-On) into a 3D printed mold. The two lateral actuators are attached to a 3D-printed rigid center using screws and 3D-printed end-caps. Below the rigid center piece, a 6-axis force/torque sensor is secured using double-sided tape.

The capacitive force/torque sensor, a variation on the work by Wu et al. [23] using the same fabrication method and an additional DoF, is 2 cm in diameter and 3.2 mm thick. It is sampled at 370 Hz. The sensor has an RMS error of 0.150 N when calibrated from 0 to 12 N in the normal direction, and an RMS error of 0.062 N when calibrated from 0 to 5 N in the shear direction. Calibration was conducted using a reference force/torque sensor (ATI, Gamma SI-32). This sensor has been used in other wearable haptic devices that produce normal and shear forces [8].

A 3D-printed assembly that encases the tactor is attached below the force sensor. This assembly has an internal channel that connects the tactor cavity, a small 2 mm space above the silicone sheet, to tubing for airflow from an external building air pressure supply. The lateral actuators are pre-stretched to allow for greater travel distance when mounted to the rigid housing [16]. The tactor provides the ability to make and break contact with the skin by pressurizing the internal cavity to make the tactor expand outward. Two pressure gauges are used for the device. One is attached to the air channels of the lateral actuators, and the other attaches to the air channels of the tactor. This allows for independent control of force normal to the skin and lateral to the skin. The pressure gauges can be adjusted to modify the maximum pressure, and thus the forces and travel distances of the actuators. Each of the three actuators has its own valve and pressure sensor which is off-board from the device (ABPDANT030PGAA5, Honeywell). The maximum normal force applied to the skin can go as high as 1.5 N and the maximum shear force is approximately 1 N, but this varies between participants based on arm size and structure.

A guide rail above the soft actuator assembly constrains vertical movement so that the tactor indents into the skin instead of raising the soft actuator assembly above the skin. The guide rail has slots allowing the tactor assembly to slide back and forth to make linear movements. Furthermore, the attachment from the tactor assembly to the guide rail constraints the motion such that the only movement of the tactor is linear across the guide rail with no bending moment. Above the guide rail is a distance sensor (Pololu, 4052, Digital Output, 10 cm range) that tracks the lateral travel distance of the tactor relative to its center position.

Rotational motion is provided by a DC motor (Pololu, 50:1, Medium-Power 6 V) attached to a 3D printed spur gear, which interfaces with a 3D printed rotational housing that contains the soft actuator assembly. When the soft assembly is mounted to the rotational housing and the tactor and lateral actuators are unpressurized (neutral position), the base of the tactor sits 0.5 cm above the skin surface at the center of the rotational housing. To position the T-shaped soft actuator assembly, the motor rotates the rotational housing containing the soft actuators and aligns them at the desired angle for the delivery of a cue. The motor system has a resolution of 0.26° and a 112.5:1 gear ratio. The maximum angular velocity is 1.5 rps, and the stall torque is 1.215 kg-cm. The motor position is determined from an encoder (Pololu, 12 CPR, 2.7–18 V), and it is controlled with a PID controller following pre-planned trajectories. The repositioning time for any motor movement is fixed at 1 s. This allows for a smooth acceleration profile to minimize inertial effects that occur during movement. All motors and valves were controlled by a Teensy 3.2 programmed in Arduino. The delay in system control for the motors and valves is less than 1 ms.

The bottom of the rigid housing is 3D printed and curved to help it conform to the arm. Rubber pads are attached to the bottom of the rigid housing for cushioning. The rigid housing also contains slots that hold Velcro straps used for fastening to the arm. These velcro straps were centered on the device, such that if the normal actuator was pressurized there would be no torques generated.Altogether, the device mass is 0.12 kg, has an outer diameter of 11.3 cm, and is 3.5 cm tall when fully assembled (Fig. 1). The sensors from the device were all connected to a DAQ (Labjack U3) for data acquisition during use.

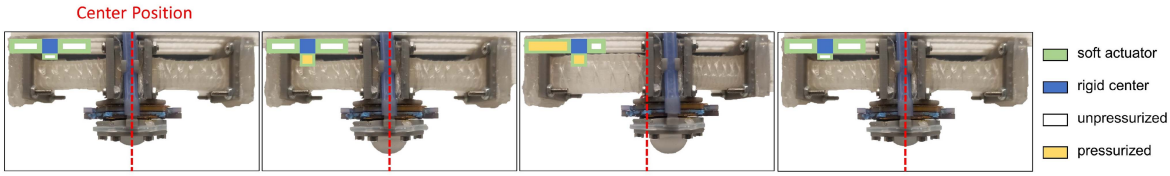

Fig. 3. Motion of the device when soft actuators are sequentially pressurized. Sequential pressurization and depressurization of the soft actuators allow for the creation of shear cues. The sequence shown here is for the Baseline condition, during which the tactor contacts the skin (not shown in this figure to give a clear view of actuator movement), followed by the pressurization of a lateral actuator to create motion in the desired shear direction. Last, the tactor and lateral actuator are depressurized, and the tactor returns to the center position. The dashed red line shows the center position and the T-shaped soft actuator assembly is shown in green and blue. Pressurized actuators are colored yellow.

III. User Studies

Two user studies were conducted to determine how effective the device is at delivering linear shear cues across four shear cue delivery conditions, as introduced in the *Device Cues* subsection. The first study tested 4 directions (4-direction task) and included 14 right-handed participants (10 Female, 4 Male, Ages 22–32). The second study tested 8 directions (8-direction task) from a different set of participants and included 14 right-handed participants (10 Female, 4 Male, Ages 21–29). The experimental protocol was approved by the Stanford University Institutional Review Board (Protocol 22514), and all participants gave informed consent.

A. Device Cues

The device was used to generate shear cues at 8 different angles (0° to 315°, in 45° increments). The DC motor controls the direction of shear delivery, while the soft actuators produce the normal and shear cues (Fig. 3). We created four conditions of shear cue delivery to test how cue speed, travel distance, and contact pattern impact perception (Fig. 4). The four shear conditions are:

- Baseline: The tactor contacts the skin, moves laterally in the direction of the desired cue, holds this position, then releases from the skin before returning to its center position.
- Larger Distance: The tactor contacts the skin, travels twice the distance of the Baseline in the direction of the desired cue, holds this position, then releases from the skin before returning to its center position.
- Contact on Return: The tactor contacts the skin, moves laterally in the direction of the desired cue, holds this position, returns to its center position, then releases from the skin.
- Shorter Time: The tactor contacts the skin, and moves laterally in the direction of the desired cue, but holds this position for half the time of the baseline, after which it releases from the skin and returns to its center position.

Shear delivery for the Baseline condition is described in Figs. 3 and 4(a). The Baseline condition begins with a 1 s movement of the rotational housing to align the soft, T-shaped actuator assembly in the angle of shear delivery. Then, after a pause of 0.5 s, the tactor is pressurized such that it contacts the skin with no lateral motion for 0.5 s. Next, a single lateral actuator is pressurized for 2 s to provide movement and a hold in the delivered cue direction, then depressurized in sync with the tactor to release contact with the skin and to move to its neutral position. Following this, the motor activates for 1 s to align the rotational housing such that the soft, T-shaped actuator assembly is in line with 0°. In the Baseline condition, the tactor initially makes contact with the skin at the center position of the device workspace. The soft actuators work in an open-loop paradigm, and all pressurization instances are step inputs. The delivered forces, movement distance, and movement speed may vary between trials and participants due to different arm sizes and mechanical properties. Subsequently, the tactor takes approximately 0.5 s to 1 s to reach the maximum cue distance of approximately 0.5 cm. It takes approximately 0.1 s for the actuator to reach its delivered pressure, and the tactor takes approximately 0.5 s to 1 s to reach the maximum cue distance of approximately 0.5 cm. The delay between the start of inflation and actual movement may vary due to the mechanical properties of the skin, but this motion is almost instantaneous because there is a high back pressure to initiate movement. An example of this movement profile is shown in Fig. 5. Due to this variation, we measured the tactor distances and forces delivered to participants during the user study.

The Larger Distance condition Fig. 4(b) differs from the Baseline condition by using both lateral actuators instead of just one. This creates coupled actuator movement, approximately doubling the tactor travel distance during the cue. In this condition, the T-shaped soft actuator assembly orients for 1 s to deliver the cue in the proper direction. Next, a single lateral actuator is pressurized to create movement away from the desired cue and held for 0.5 s without touching the surface of the skin. Then, the center actuator is pressurized to contact the skin with no lateral motion for 0.5 s. To create shear force, the other lateral actuator (that elongates in the desired direction of the shear) is pressurized for 2 s in sync with the depressurization of the opposing lateral actuator to provide the cue. This coupled pressurization in the desired direction and depressurization in the opposing direction helps to create a larger travel distance. After this, the actuators are depressurized in sync with the normal actuator to release contact with the skin and move to the center position. Then, the motor activates to return the housing to its center position for 1 s. In this cue condition, the tactor has contact with the skin for 2.5 s, the same as the Baseline condition. The total time holding the cue in the delivered direction is also the same as the Baseline

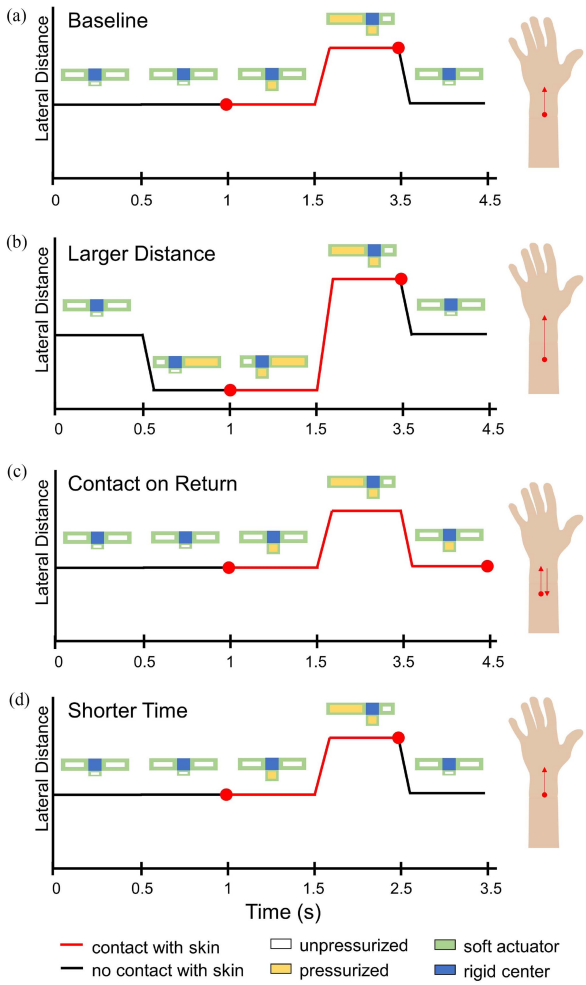

Fig. 4. Cue delivery conditions. These plots show the lateral distance and phasesof skin contact (red) for the different cue conditions. Four conditions were compared to a Baseline (a) to see how a Larger Distance (b), Contact on Return (c), and Shorter Time of a cue (d) impact perception. The cross-section of the T-shaped soft actuator assembly is shown in green and blue. Pressurized actuators are colored yellow. The arrows on the arms indicate the tactor movements along the skin, with the red circle being the point at which the actuator contacts the skin.

condition, 2 s. However, due to the coupled motion, the tactor travel distance is approximately 1 cm instead of 0.5 cm (each soft actuator can generate about 0.5 cm of motion).

The Contact on Return condition Fig. 4(c) differed from the Baseline condition by having the tactor maintain contact with the skin during all lateral movements. This exemplifies the motion that would have been obtained similar to a prior study [16], and other 2-DoF shear displays [5]. For this condition, contact time increases. In this condition, the tactor is pressurized, to touch the skin for 0.5 s. Next, a single lateral actuator is pressurized for 2 s to provide movement and a hold in the delivered direction. Unlike the baseline, the tactor continues to have contact with the skin for an additional 1 s as the lateral actuator depressurizes so that the tactor returns to the center. Subsequently, the tactor depressurizes to remove contact with the skin. Following this, the motor returns the housing to its center position for 1 s. In this cue condition, the tactor has contact with the skin for 3.5 s (1 s longer than the baseline), and has an overall travel distance of approximately 1 cm, with 0.5 cm going in the direction of the linear cue, and 0.5 cm going in the opposite direction of the cue upon tactor return.

The Shorter Time condition shortened the amount of time that the lateral actuator is pressurized from 2 s to 1 s, thus reducing the overall time of the cue at its final position compared to the baseline Fig. 4(d). This results in a total travel distance of approximately 0.5 cm in the direction of the delivered cue. This was tested to see if cue duration impacts perception.

Sample data from a single cue shows how the motor position and actuator pressures result in a change in tactor lateral distance, shear, and normal forces Fig. 5. When shear force was delivered to the skin, it peaked at the onset of lateral pressurization, then slowly declined and plateaued as lateral distance increased and stabilized. Importantly, the plots show no changes in shear force, normal force, and lateral distance during the movement of the motor, meaning that when the housing moves, there is no contact or forces being delivered by the tactor to the skin.

While the soft actuators have all components allowing for closed-loop force or distance control, we conducted our user studies using open-loop control due to hardware limitations and feedback from pilot participants. Due to non-linear materials and low bandwidth pressure regulators, closed-loop control of the soft actuators was difficult. Additionally, the solenoid valves with binary toggles for the pressure created very noticeable vibrations that detracted from the cue itself, even when used at their maximum control frequency.

B. Protocol

The device was mounted to the participant such that the tactor was located on the left dorsal forearm, with the end of the rigid housing placed just proximal to the wrist joint. Before the study, the tightness of the Velcro band used to attach the device was normalized across all participants. This was done by placing a 0.5 cm 3D-printed spacer under the tactor (since the tactor clearance when unpressurized is 0.5 cm above the skin) and tightening the Velcro until the force sensor read 1.0±0.05 N.

Next, the participant placed their arm on a pillow with a cut-out that kept the arm and hand aligned such that there was no wrist rotation. This arm position remained constant throughout the remainder of the calibration and user study. Next, the tactor pressure was increased until the device provided a normal force of 0.5 N when touching the skin. While the tactor was still pressurized and contacting the skin, the lateral pressure was increased until the tactor would displace by 0.5 cm. After calibration, a curtain blocked the participant's view of the device for the duration of the study.

The cue angle definitions are shown in Fig. 6. In this study, the 0° cue is parallel to the forearm and in line with the middle finger. The 180° direction was parallel to the forearm towards the elbow. The 90° direction was perpendicular to the forearm toward the thumb, while the 270° direction was perpendicular to the forearm toward the pinky. The 4-direction task included

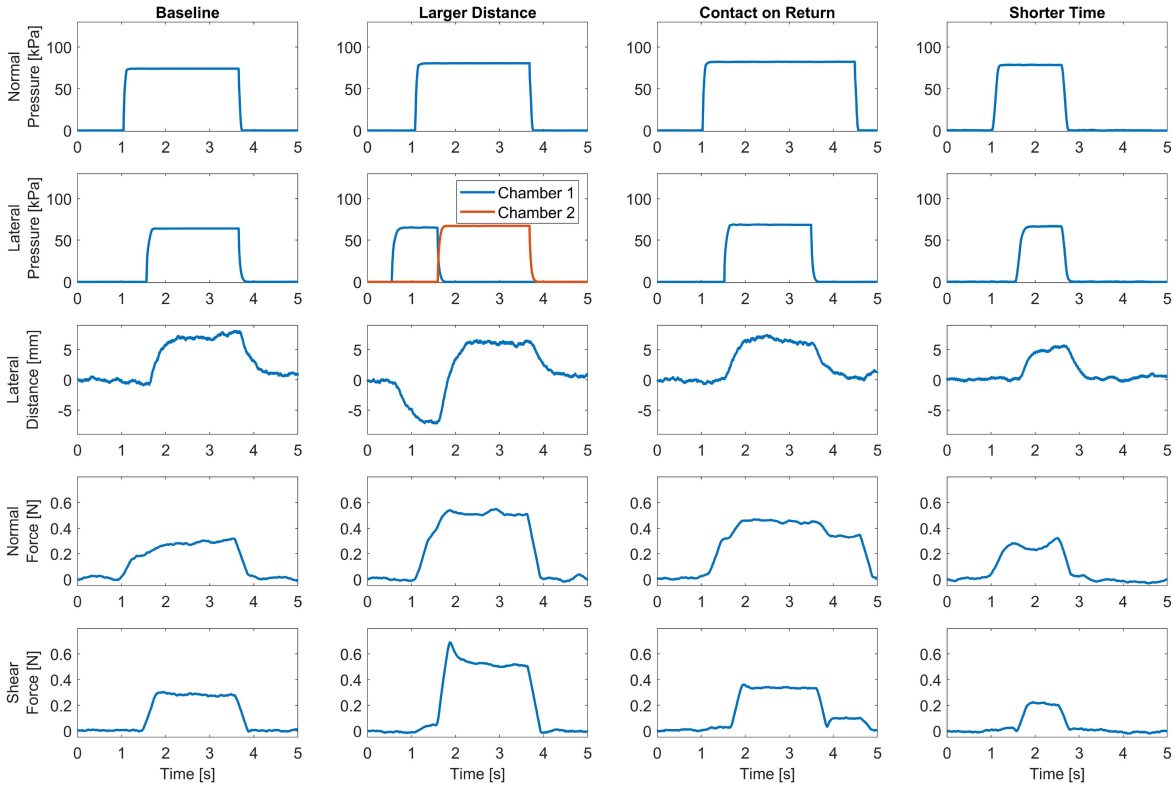

Fig. 5. Examples of pressure, lateral distance, and force data from a single trial for each condition. Pressure, lateral distance, and force data were collected to understand the device performance on participants. When a cue is delivered, the motor position changes to align the tactor in the direction of the cue to be delivered. Next, the soft actuators are pressurized to produce normal and shear force on the skin. Lateral distance increases and decreases in sync with lateral pressure.

cues at 0°, 90°, 180°, and 270° directions. The 8-direction task included 0°, 45°, 90°, 180°, 225°, 270°, and 315°.

After calibration, the participants used a graphical user interface to input responses. This interface guided participants through three sections: an open exploration phase, a practice phase, and an experimental phase. During the exploration phase, participants clicked buttons to feel directional cues. The participants had to feel each directional cue at least twice before moving on to the practice phase. During this exploration phase, participants were instructed to take time to learn how the cues felt, so they could identify them in the experiment. After the exploration phase, the practice phase provided one of each cue in a random order to the participant. The participant clicked a button to start a cue and then clicked on the cue that they perceived. In the practice phase, participants were provided with the correct answer to help ground their responses. Lastly, in the experimental phase, participants completed 3 trials for each delivered direction but received no feedback as to whether their response was correct or incorrect. There were 12 trials for the 4-direction task and 24 trials for the 8-direction task. Participants were provided each set of cues in a pseudo-random order such that each direction was given once before being repeated.

The exploration, practice, and experimental phases were repeated once for each cue condition, for a total of four times, once for each condition (Fig. 4). The order in which participants received the cue condition was pseudo-randomized such that no two participants received the same order.

After experiencing each cue condition, participants were asked to state how difficult the task was in general on an easy-to-difficult scale (1–5). After completing the full experiment, participants were asked to complete a post-experiment survey which evaluated the mental demand, physical demand, temporal demand, performance, effort, and frustrationon a scale from 1 to 10. This survey was a modified version of the NASA TLX Questionnaire, such that the ratings go from 1 (low) to 10 (high) for all categories (i.e., a performance score of 10 means that the subject thought they did very well). Participants were also asked to describe any strategies they used to complete the task in addition to any other comments they had about the study or the device.

C. Statistical Analysis

User performance was measured by examining *accuracy*, *angular error*, *response time*, *difficulty*, and *angular bias*. *Accuracy* is the percentage of correct responses. *Angular error* is the average of the absolute difference between the delivered and participant-identified angle. *Response time* was a measure of the time it took for the participant to respond after a cue was delivered. *Difficulty* is a measure on a 5-point scale from easy

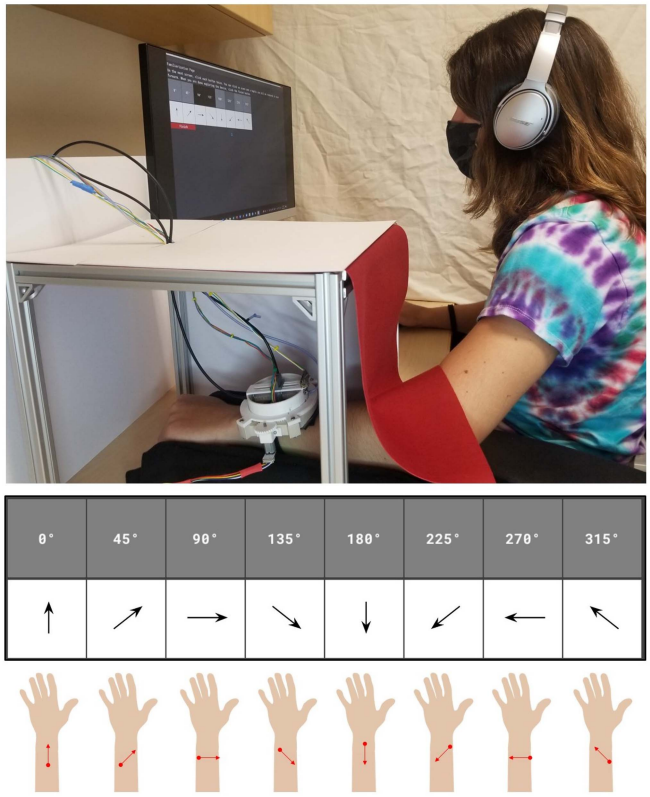

Fig. 6. User study setup. Participants wore the device on the left dorsal forearm and responded via a graphical user interface to identify which stimulus angles were felt. Participants were asked to identify cues from a set of four angles (0°, 90°, 180°, 270°) in the 4-direction task and eight angles in the 8-direction task (0° to 315°, in increments of 45°). 0° is defined as towards the middle finger, and 180° oriented towards the elbow. Participants listened to white noise through noise-cancelling headphones, and their arm was covered during the experiment.

to hard (1 to 5). *Angular bias* was calculated as the average difference between the stimulus axis and the response axis (if a participant selected the angle opposite of the stimulus angle, then there would be no *angular bias*). This provided a measure of any spatial preference for responding to the cues. *Angular variance* is the variance of the *angular bias* from a single participant.

Normal force, *shear force*, and *lateral distance* were measured during the 4-direction task to evaluate device performance. *Normal force* and *shear force* correspond to the maximum normal force or shear force created during a cue. The *lateral distance* is the mean tactor travel distance when a single actuator is pressurized. Thus, for the Larger Distance condition, we divided the total measured travel distance by two to get the average travel distance for a single actuator.*Normal force variance*, *shear force variance*, and *lateral distance variance* were calculated as the variance of each measure for a given participant. The variance provides a metric on how much the pressures, forces, and distances varied within a particular participant throughout the study. Thus, if the variance metric is high, this means that there is large variability in the forces, pressures, or distances being delivered by the device between trials on the same participant.

The Friedman's test was used to compare the non-parametric measures of *accuracy*, *angular error*, and *difficulty* between the conditions. When the Friedman's test yielded significant results, a post-hoc analysis was conducted using the Wilcoxon signed rank test.

A one-way repeated measures ANOVA was used for parametric measures including delivered *normal force*, *shear force*, *lateral distance*, *response time*, and *angular bias* in addition to the variances of these measures. Mauchly's test for sphericity was used to confirm compound symmetry. When sphericity did not hold, the Greenhouse-Geisser adjustment was used to correct the p-value. Post-hoc analysis was conducted using pairwise T-tests with Bonferroni correction to identify significant differences between conditions. Unpaired T-tests were used to compare the survey data between different conditions.

All statistical analyses were conducted using MATLAB and the Statistics and Machine Learning Toolbox (Mathworks).

IV. Results

Four cue conditions were tested during the 4-direction and 8-direction task. *Accuracy*, *angular error*, *response time*, and *difficulty* were used to quantify participant performance. Distance, pressure, and force measurements were used to quantify device performance in the 4-direction task.

A. User Performance

The confusion matrices for the 4-direction task show the percentage of correct responses for each stimulus angle for all cue conditions (Fig. 7). The most salient cue in the 4-direction task occurred in the Larger Distance condition (90% *accuracy* in the 180° direction). The least salient cue occurred in the Shorter Time condition (52% *accuracy* in the 180° direction). Across all conditions, participants had the lowest *accuracy* for cues in line with the long axis of the arm (0° or 180°). For most conditions, the cue with the highest *accuracy* was along the minor axis of the arm (90° or 270°). In the 4-direction task, incorrect participant responses were most common for the cue in the opposite direction (180° offset). For example, in the Contact on Return condition, 23% of 180° cues were perceived as 0°, and 21% of 0° cues were perceived as 180°.

Participants had a lower *accuracy* when identifying cues from a set of 8 directions compared to 4 directions for all conditions (Fig. 8). The most salient cue in the 8-direction task occurred in the Baseline condition (59% *accuracy* in the 90° direction), and the least salient cue occurred in the Contact on Return condition (19% *accuracy* in the 135° direction). Unlike the results from the 4-direction task, the 8-direction task shows confusion predominantly with angles next to the stimulus. This is shown by the distribution of incorrect responses around the diagonal where the stimulus and perceived angles match. For instance, in the Baseline condition, when 135° is delivered, 37% of responses identify the cue directly next to it (either 90° or 180°), while just 7% of responses identify the cue opposite of it (315°).

Bar graphs showing the mean *accuracy* , *angular error* , *response time* , and *difficulty* for the 4-direction and 8-direction tasks are shown in Fig. 9.

1) Accuracy: The Larger Distance condition had the highest *accuracy* in the 4-direction task (85.1%). Average *accuracy* for

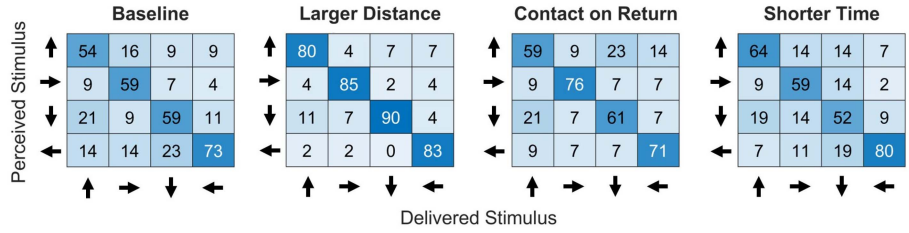

Fig. 7. Confusion matrices for the 4-direction task. User response percentages are shown in these confusion matrices. Most participant responses centered on the diagonal, indicating matches between delivered and perceived angles. The Baseline, Contact on Return, and Shorter Time conditions show more variability in response compared to the Larger Distance condition.

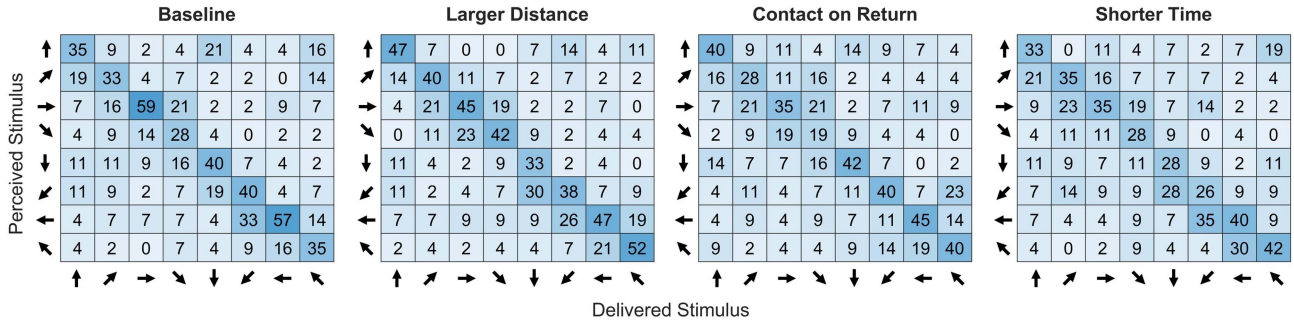

Fig. 8. Confusion matrices for the 8-direction task. User response percentages are shown in these confusion matrices. The Baseline condition has the most easily detectable cue of 90°. The Contact on Return and Shorter Time conditions showed more variability in response compared to the Larger Distance condition.

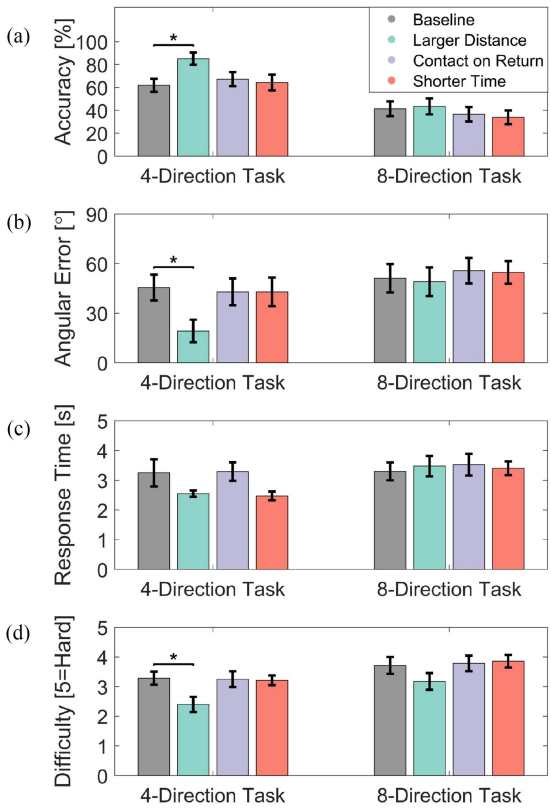

Fig. 9. User Performance. These bar graphs show the *accuracy*, *angular error*, *response time*, and *difficulty* for four cue delivery conditions for the 4-direction task and 8-direction task. The Larger Distance condition had a higher *accuracy*, lower *angular error*, and lower *difficulty* than the Baseline. There were no significant differences between the Baseline and any other conditions in the 8-direction task. (*=p<0.05).

participants ranged from 25% to 100% across all conditions, with the lowest performing participants scoring an *accuracy* equal to random chance. A Friedman's Test revealed that *accuracy* in the 4-direction task was statistically significantly different between the conditions ($\chi^2 = 17.0$, $p = 7.01 \times 10^{-4}$, W = 0.405). A pairwise Wilcoxon signed rank test between the conditions revealed statistically significant differences between the Baseline and the Larger Distance condition (p = 0.014).

The Larger Distance condition had the highest *accuracy* in the 8-direction task (43.5%). Average *accuracy* for participants ranged from 12.5% to 100%, with the lowest performing participants scoring an *accuracy* equal to random chance. A Friedman's Test found no differences in *accuracy* between any conditions in the 8-direction task ($\chi^2 = 2.98$, p = .395, W = 0.078).

2) Angular Error: The lowest *angular error* in the 4-direction task occurred in the Larger Distance condition (19.3°). Average *angular error* for participants ranged from 0° to 97.5°. A Friedman's Test revealed that *angular error* in the 4-direction task was statistically significantly different between the conditions ($\chi^2 = 17.6$, p = 5.20×10^{-4}, W = 0.420). A pairwise Wilcoxon signed rank test between the conditions revealed statistically significant differences between the Baseline and the Larger Distance condition (p = 0.015).

The lowest *angular error* in the 8-direction task also occurred in the Larger distance condition (49.0°). Average *angular error* for participants ranged from 0° to 120° in the 8-direction task. A Friedman's Test found no differences in *angular error* between any conditions in the 8-direction task ($\chi^2 = 0.116$, p = 0.990, W = 0.003).

3) Response Time: The average *response time* in the 4-direction task was lowest for the Shorter Time condition (2.5 s)

and highest for the Contact on Return condition (3.3 s). *Response time* for participants ranged from 3.1 s to 8.2 s in the 4-direction task. A one-way repeated-measures ANOVA found that there was a statistically significant difference in *response time* between the conditions in the 4-direction task ($F(1.68, 21.8) = 3.687$, $p = .049$, $\eta_p^2 = 0.221$). However, post-hoc analyses with a Bonferroni adjustment revealed that there were no conditions were different from the Baseline.

The average *response time* in the 8-direction task was lowest for the Baseline condition (3.3 s) and highest for the Contact on Return condition (3.5 s). *Response time* for participants ranged from 1.9 s to 6.8 s in the 8-direction task. A one-way repeated-measures ANOVA found that there were no statistically significant differences in *response time* between the conditions in the 8-direction task ($F(3, 39) = 0.284$, $p = .836$, $\eta_p^2 = 0.006$).

4) Difficulty: Participants rated the Larger Distance condition as the easiest for both the 4-direction and 8-direction tasks. A Friedman's Test revealed that *difficulty* in the 4-direction task was statistically significantly different between the conditions ($\chi^2 = 15.0, p = 1.84 \times 10^{-3}, W = 0.356$). A pairwise Wilcoxon signed rank test between the conditions revealed statistically significant differences between the Baseline and the Larger Distance condition ($p = 0.026$). A Friedman's Test revealed that there were no significant differences in *difficulty* between the conditions in the 8-direction task ($\chi^2 = 7.31$, $p = 0.063$, $W = 0.174$).

5) Angular Bias and Variance: Angular bias was calculated as the average difference between the stimulus axis and the response axis (if a participant selected the angle opposite of the stimulus angle, then there would be no *angular bias*). This provided a measure of any spatial preference for responding to the cues. *Angular variance* was determined by averaging the variance of the *angular bias* from each participant.

Participants had a 15.53° clockwise *angular bias* for cues in the 45° direction, and a 17.14° clockwise *angular bias* in the 225° direction (Fig. 12). This means that when participants were provided a 45° stimulus, they would often interpret it as a cue closer to 90°, and that when participants were provided a 225°, they would often interpret it as a cue closer to 270°. The 0° direction showed the smallest *angular bias*. A one-way repeated measures ANOVA revealed that the *angular bias* was not different for any particular stimulus angle ($F(7, 91) = 1.00$, $p = 0.064$, $\eta_p^2 = 0.133$).

The average *angular variance* averaged around 6°. The *angular variance* across stimulus angles is small and constant, with no single angle having more variance than another, meaning that overall, participants had equal uncertainty in selecting angles and often selected angles next to the stimulus angle. A one-way repeated measures ANOVA revealed that the stimulus angle has a statistically significant effect on *angular variance* ($F(7, 91) = 5.07$, $p = 6.83 \times 10^{-5}$, $\eta_p^2 = 0.28$). Post-hoc analyses with a Bonferroni adjustment revealed that there was a significant difference in variance between 0° and 225° ($p = 0.032$).

6) Survey Data: Fig. 10 shows the results from the questionnaire provided to participants. An unpaired t-test comparing the 4-direction task and 8-direction task for mental demand, physical demand, temporal demand, effort, and frustration showed no significant differences (A separate t-test was conducted for each variable). Participants reported that they performed better on the 8-direction task compared to the 4-direction task ($p = 0.021$, $t = -2.451$, $d = -0.899$).

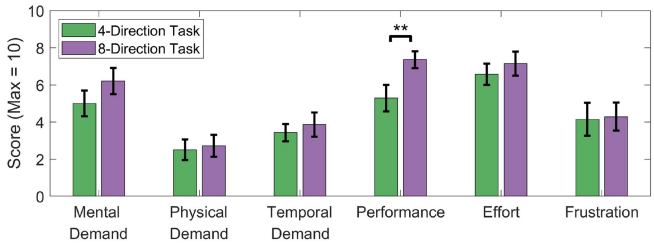

Fig. 10. Survey Results. Mean and standard error of participant responses to the task load index survey. Participants scored the 4-direction task and 8-direction task similarly but reported that they performed better on the 8-direction task. (**=p<0.01).

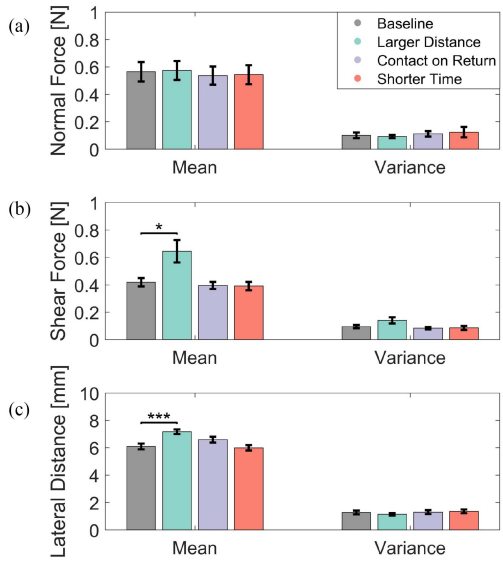

Fig. 11. Device Metrics from the 4-direction task. a) The device delivered a similar mean *normal force* across all conditions. The *normal force variance* quantified the consistency of the delivered *normal force*. b) The device delivered a higher *shear force* for the Larger Distance condition. The *shear force variance* quantified the consistency of the delivered *shear force*. c) *Lateral distance* measures tactor movement created by a single acutator. In the Larger Distance condition's coupled actuator configuration, the device created a larger *lateral distance*.The *lateral distance variance* quantified the consistency of the delivered *lateral distance*. (*=p<0.05, ***=p<0.001).

B. Device Performance

Device data taken during the 4-direction task, including *normal force*, *shear force*, and *lateral distance* are shown in Fig. 11.

1) Normal Force: The average *normal force* delivered to participants was lowest for the Contact on Return condition (0.54 N) and highest for the Larger Distance condition (0.57 N). These values are higher than thetargeted *normal force* used for calibration Fig. 11(a). A one-way repeated measures ANOVA found that *normal force* was not different between the different conditions ($F(1.7, 22.15) = 0.643$, $p = 0.511$, $\eta_p^2 = 0.047$).

The average *normal force variance* measured the variance of *normal force* for participants throughout the study. *Normal*

force variance provides a metric to quantify the consistency of the *normal force* being delivered. The *normal force variance* was within 25% of the average *normal force* for all conditions at around 0.1 N. A one-way repeated measures ANOVA found that *normal force variance* was not different between the different conditions ($F(1.4, 28.21) = 0.886$, $p = 0.394$, $\eta_p^2 = 0.064$).

2) Shear Force: the Larger Distance condition resulted in the highest *shear force* (0.65 N) as shown in Fig. 11(b). A one-way repeated measures ANOVA found that *shear force* was different between conditions ($F(1.41, 18.35)=4.36 \times 10^{-4}$, $p = 0.511$, $\eta_p^2 = 0.533$). Post-hoc analyses with a Bonferroni adjustment revealed that there was a significant difference in *shear force* between the Baseline and Larger Distance conditions ($p = 0.017$).

The average *shear force variance* measured the variance of *shear force* for participants throughout the study. *Shear force variance* provides a metric to quantify the consistency of the *shear force* being delivered. The *shear force variance* was within 25% of the average *shear force* for all conditions. A one-way repeated measures ANOVA found that *shear force variance* was different between the different conditions ($F(3, 39) = 5.752$, $p = 0.002$, $\eta_p^2 = 0.307$). However, post-hoc pairwise comparisons with a Bonferroni adjustment revealed that there was no significant difference in *shear force variance* between conditions.

3) Lateral Distance: The *lateral distance* shown in Fig. 11(c) is the mean tactor travel distance for a single actuator when it is pressurized. For all conditions except the Larger Distance conditions, only one actuator is pressurized to produce the directional cue. In contrast, the Larger Distance condition has a larger linear cue distance by using two actuators using coupled actuator movement. In addition to having two actuators produce movement, the data show that each of these actuators also generates larger individual distances when coupled Fig. 11(c).

The Larger Distance condition had the highest *lateral distance*, the distance created by a single actuator, 7.16 mm. This means that for the Larger Distance condition, the total travel length across the skin averaged to be 14.32 mm, since two actuators are activated in this condition. A one-way repeated measures ANOVA found that *lateral distance* was different between conditions ($F(3, 39)=16.369$, $p = 4.84 \times 10^{-7}$, $\eta_p^2 = 0.557$). Post-hoc analyses with a Bonferroni adjustment revealed that there was a significant difference in *lateral distance* between the Baseline and Larger Distance conditions ($p = 8.40 \times 10^{-4}$).

The average *lateral distance variance* measured the variance of *lateral distance* for participants throughout the study. *Lateral distance variance* provides a metric to quantify the consistency of the *lateral distance* being delivered. The *lateral distance variance* was within 25% of the average *lateral distance* for all conditions. A one-way repeated measures ANOVA found that *lateral distance variance* was not different between the different conditions ($F(3, 39) = 0.835$, $p = 0.483$, $\eta_p^2 = 0.060$).

V. Discussion

A. User Performance

Participants had an 85.1% *accuracy* in the 4-direction task, similar to the previous 2-DoF device's [16] *accuracy* of 86%.Our device *accuracy* is lower than WRAP, which had an *accuracy* of 99.4% [13]. In contrast to WRAP, the directional cues from our device are delivered in a single contact point through shear, rather than a distributed contact point through normal indentation around the wrist. The *response time* found in our study is on par with WRAP, which ranges from 2–3 s [13]. A rigid 2-DoF analog of our device [5] with a rigid tactor and servo motors had recognition ratesslightly less thanour device, with the ability to recognize five shear patterns with an *accuracy* of 72% to 78% on the forearm.The shear patterns on this 2-DoF, rigid device consisted of drawing shapes and two linear cues, while our device only provided linear cues in different directions. The higher accuracy on our device may result from the ability to make and break contact with the skin or the difference in the cues provided to the users during the experiment. When repeated cues are provided, it can also be difficult to interpret the end of one cue and the beginning of the next, so our device offers a way to use skin contact to identify sequential cues. The use of pneumatic actuation on our device allows for a softer touch and enhanced safety with less concern over an actuator causing harm or discomfort due to erroneous movements. The pneumatic system also enables faster actuator motion compared to those used by Kuang et al. [5].

Kuniyasu et al. developed a device that provides 2-DoF shear on both sides of the forearm simultaneously with a correct answer rate greater than 90% for four directions [3]. Our device, which stimulates the skin on only one side of the forearm, had a lower *accuracy* , showing that stimulation on just one side may result in decreased *accuracy* . Caswell et al. showed that an externally grounded device could produce an 89% *accuracy* for perceiving four directional cues [6]. Although our device *accuracy* is slightly lower, it demonstrates the feasibility of transferring the capabilities of a robust, externally grounded system to a forearm-mounted, wearable device.

Participants performed poorly on the 8-direction task (43.5% *accuracy*). While this is still better than chance (12.5% *accuracy*), perceptual limits, grounding, cue interference, tactor material, and device placement may all be factors contributing to device performance.

1) Perceptual Limits: Previous pilot data from our lab [16], found that 1 mm of skin displacement from a rigid, miniature 3-DoF tactor results in an average *angular error* of 30° when participants were asked to select from 4 directional cues. Our device has a larger displacement (6–7 mm), but only shows a relatively low improvement in average *angular error* (19.3°). Another study [24] that assessed shear *accuracy* used a Phantom Premium device to deliver directional shear cues in 8 directions on the neck, yielding a 65.6% *accuracy* ($n = 1$) for a single, highly-trained participant. This is higher than our average *accuracy* from the 8-direction task, likely because the device uses closed-loop control, uses a rigid factor, and operates in an area known to have better perception thresholds compared to the forearm [25]. However, this 65.6% *accuracy* still seems relatively low, considering that perception of shear in four directions on the forearm, where tactile perception would be worse, can be as high as 90% [3]. Because of the limited improvement in accuracy when having a higher cue distance or by having a

highly-controlled rigid device with a trained participant, these studies suggest that there may be limitations in angular perception on the skin, partially explaining the poor performance in the 8-direction task.

The survey difficulty ratings also suggest that perception limits may have been reached since participants found the 8-direction task more challenging, in addition to the increase in *angular error* and drop in *accuracy*. This indicates the struggle to discern cues from the sparse mechanoreceptor forearm distribution [12]. The higher *difficulty* scores in the 8-direction task may be evidence of the increased cognitive load to determine an outcome based on sparse information. Future work should examine shear angle discrimination on the forearm, as work in this area is very limited.

The surveys showed that there were similar mental demands, physical demands, temporal demands, effort, and frustration from the 4-direction and 8-direction tasks. However, participants thought that they performed better in the 8-direction task than in the 4-direction task. This could be because the 8-direction task had more intermediate options, allowing participants to select angles that they felt were at least near correct, rather than having a larger margin of error from the less-continuous 4-direction task options. To assess the general difficulty of using the device, we can compare these scores to another study that evaluated demands from using a mobile phone [26]. The device has similar demands to perceiving vibrations from a mobile phone, however, participants from this study reported a much higher effort and a higher mental demand needed to perceive shear. This may show that perceiving shear on the forearm has additional difficulties compared to perceiving simple phone vibrations at the fingertips.

2) Force Grounding: Reaction forces transmitted from our device to the forearm may have also led to participant confusion. Many fingertip haptic devices [1] are grounded on rigid portions of the body (such as nails or joints), allowing for adequate force grounding and higher accuracies at the fingertip.However, when the device is grounded on a soft surface like the forearm near the location in which the cues are being delivered, there can be difficulty in perception due to interference from reaction forces. For instance, when the tactor moves in one direction on the skin, there will be a reaction force from the device that moves in the opposite direction, thus causing confusion. This can explain why many of the incorrect responses in our user study were in the opposite direction of the stimulus angle and why the *angular bias* significantly drops compared to the *angular error*. Thus, future wearable devices should focus on minimizing confounds when delivering cues and might benefit from having larger contact areas to distribute reaction forces.

3) Cue Interference and Device Materials: Furthermore, the forces from fastening the device can create a masking squeeze effect that interferes with the perception of the shear cues [27]. When our device is fastened to the wrist, the velcro attachment and the normal indentation of the tactor create a squeeze, which can interfere with the ability to perceive the shear cue. In contrast to other wearable devices for the forearm, our device has a soft tactor which may have increased confusion in cue discrimination. The soft, compliant tactor conforms to the skin with a changing contact area, which may have resulted in the large variations (25%) in *normal force* created by the device.

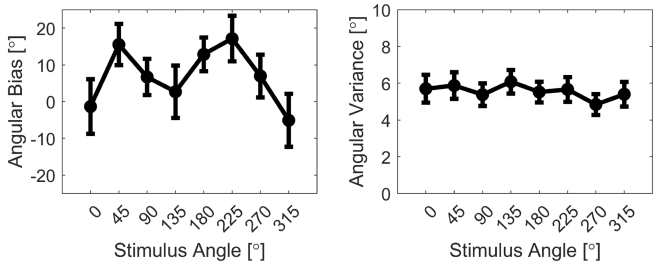

Fig. 12. Angular Bias and Variance. *Angular bias* is calculated as the mean difference between the stimulus and response angle axis. A positive *angular bias* means that a subject had a preferential response for a cue in the clockwise direction, and a negative *angular bias* corresponds to a bias in the counterclockwise direction. Participants have a strong positive *angular bias* centered about the 45° and 225° angles, meaning that participants tended to more commonly select angles at 90° and 270° for these stimuli, respectively. At 0° and 315°, participants have less bias in their response, meaning that on average, they select the correct direction. *Angular variance* is metric on the spread of the *angular bias* within each participant. Participants had a small and consistent amount of angular variance meaning that most confusion about the stimulus angle was consistent and near the correct angle.

4) Device Placement: Similar to Kuroki et al. [28], we found that there exists a small *angular bias* when cues are applied to the forearm. These biases exist, despite having all participants keeping their arms straight and having the device calibrated for alignment. The two largest *angular biases* occurred for 45° or 225°, and both move towards the minor axis of the arm (towards 90° or 270°). Notably, in our study, the minor axis showed higher *accuracy* compared to the major axis. Other studies have also found that there is more accurate localization along the minor axis of the arm as opposed to longitudinally, which might also result in the bias to respond in this axis [29]. Furthermore, the small *angular bias* for 135° and 315° matches other work [28] that shows that errors tend to be made towards 'anchor points' which for the wrist would be the wrist joint. Thus, for cues on the 135°/315°, it would also make sense that there would be a smaller *angular bias* present.

From this *angular bias* data, we can also determine if the DC motor on the device was calibrated properly. The DC motor uses relative positions, so prior to the experiment, it had to be calibrated for all participants. The *angular biases* do not have a constant, steady offset for all angles, which would have indicated a systematic calibration or alignment error with the device itself.

Because the device is primarily fastened via the major (via the rigid mount) and minor axis (via a strap) of the arm, any movement of the device with respect to the wrist during a cue would also generate more errors in the diagonal directions. For instance, if the device happens to move during any cues along the major or minor axis of the arm (along the anchoring axes), then the result would just be a reduced stimulus in that direction. However, if the device moved during a diagonal cue, then the reaction forces would cause the device to move in two components in the opposing major and minor axis, causing additional confusion for the user and lower angular accuracies. This could also be a large contribution to the angular biases in the diagonal directions (Fig. 12).

Our quantitative results support that there may be biases present on the arm, and these match up with some participant comments. One participant said that most of the cues would "feel like 315°" while another said that "everything felt like 270°". Two participants also commented that "0° and 180° were harder" and one participant said that they would try to "feel a pull on the joint where the hand connects to the forearm." These comments further support the idea of varied spatial acuity based on the cue direction on the arm and that there may be participant bias towards 'anchor points' such as the ulnar styloid process which was situated near where the device was attached.

B. Cue Conditions

We hypothesized that the Larger Distance condition would improve *accuracy* and that the Contact on Return and Shorter Time conditions would impair *accuracy*. We hypothesized that the *response time* and *difficulty* scores would show a similar trend with *accuracy*.

The Larger Distance condition was the only condition showing significant differences from the Baseline and all other conditions for both *accuracy* and *angular error*. While the Larger Distance condition had a larger tactor travel path, it also had a higher *shear force*. Thus, it could be that the control pattern for the actuators in the Larger Distance condition creates an environment with higher *shear force* that allows for better performance for the participant. Recent work has shown that the method of shear cue conveyance (using either closed-loop position or force control schemes) can affect perceptual performance, with higher perceptual resolution observed for cues that were position-controlled [30]. Given that our system works on an open loop paradigm, it is still unclear whether *shear force* or *lateral distance* is the significant factor that results in increased *accuracy* in our experiments, as both increased *shear force* and increased *lateral distance* coincided with increased *accuracy*. In addition to having a higher *accuracy*, the Larger Distance condition also had an *angular error* almost half that of all the other conditions, a trend for a faster *response time*, and lower *difficulty*.

The Contact on Return condition was similar to the previous device [16], in which the tactor would continuously have contact with the skin both in the direction delivered to the participant and the return direction to the center. It was hypothesized that the return motion creates confusion for the participant and results in decreased *accuracy* and high response rates for incorrect cues in the opposite direction. Contrary to our expectations, the Contact on Return condition was not different from the Baseline, showing that this parameter does not significantly impact *accuracy*, *angular error*, or *difficulty*. Furthermore, this condition did not result in differences in *shear force* or *normal force* with the Baseline. Because this contact pattern did not result in any significant differences from Baseline, this also suggests that the reason for the poor response rate is not from the confusion on tactor return, but another reason such as perceptual limits or force grounding. Given that the Contact on Return and Baseline conditions performed similarly, one might expect that a 2-D device that maintains contact with the skin would suffice. However, because the Larger Distance condition shows improvement over the baseline, it is clear that the third degree of freedom on the device to make and break contact with the skin is necessary. If the device had only 2-DoFs, then it would not be possible to create the Larger Distance condition, as it uses coupled motion that relies on timed contacts and breaks from the skin.

Lastly, participants had an easier time understanding cues from the Shorter Time condition. Similar to another study that investigated the impact of cue presentation velocity on skin stretch perception [31], we found that a shorter cue duration does not have a significant impact on perception, *response time* or *difficulty*. Prior work [31] also suggests that participants would rate faster cues as easier to discern, but those results were not present in our study, which might be because our study does not control the actual delivery velocity of the cue, but rather the overall cue time for the Shorter Time condition.

C. Device Performance

Many rigid haptic devices have force or position control to ensure consistent delivery of cues [17], [30], [32], but when designing pneumatic devices for haptic feedback, closed-loop control can be difficult due to limitations in bandwidth from the material properties of the actuator and the pneumatic system. We integrated a distance, force, and pressure sensor into our device to better understand how the device interacts with the skin and to assess any need for closed-loop control of the pneumatic system.

In a similar experiment to ours, using a force-controlled Phantom Premium haptic device externally grounded, it was found that commanding a 0.5 N *shear force* with a force-control scheme results in a 0.1 N average error which corresponds to 20% of the commanded force [24]. Our device operates on an open-loop paradigm when delivering shear, and we similarly found a 0.1 N variance with an average *shear force* of about 0.5 N. Thus, even when operating on an open-loop system, it appears that the device can create consistent and repeatable cues ideal for perception akin to a desktop commercial haptic device. Furthermore, *lateral distance variance* is also around 20% of the mean *lateral distance*, showing that the *lateral distances* are also consistent and repeatable for each participant. Because pressure controllers have low bandwidth, it is promising to see that a simple valve-regulator system can create consistent pressures that result in repeatable cues on par with a phantom premium.

However, this device may still benefit from the integration of closed-loop control for the soft actuators. While we did not use closed loop control due to limitations in bandwidth, in the future, a device could be created that uses a pump instead of valves so that there is a smoother delivery of air pressure while also delivering salient tactile cues.

Because of different forearm sizes and skin mechanical properties, closed-loop control could be used to deliver controlled velocity profiles to enhance cue saliency. In the current device format, we used valves to rapidly increase pressure to create lateral movement, but the lateral motion has a lot of stiction and friction that can cause irregularities in cue delivery (Fig. 5). Closed-loop control to deliver a more consistent or constant velocity could aid in the delivery of the cue.

VI. Conclusion and Future Work

This work introduced a new haptic device that delivers linear shear cues on the forearm. We tested four cue conditions in a 4-direction and 8-direction task and found that a larger contact distance and shear force results in more salient cues. Using an on-board pressure sensor, distance sensor, and custom force sensor, we found that the device has consistent *shear force* and *lateral distance* outputs, despite working on open-loop control. Future wearable haptic devices can incorporate directional shear and develop new soft actuators to produce more types of cues on the forearm. In the future, we will work on a new device to fit in a smaller form factor and to examine different ways to use shear in haptic applications. Furthermore, we will analyze the just noticeable difference for angle discretion on the forearm with a force and distance controlled setup.

References

[1] C. Pacchierotti, S. Sinclair, M. Solazzi, A. Frisoli, V. Hayward, and D. Prattichizzo, "Wearable haptic systems for the fingertip and the hand: Taxonomy, review, and perspectives," *IEEE Trans. Haptics*, vol. 10, no. 4, pp. 580–600, Oct.–Dec. , 2017.

[2] O. Kayhan, A. K. Nennioglu, and E. Samur, "A skin stretch tactor for sensory substitution of wrist proprioception," in *Proc. IEEE Haptics Symp.*, 2018, pp. 26–31.

[3] Y. Kuniyasu, M. Sato, S. Fukushima, and H. Kajimoto, "Transmission of forearm motion by tangential deformation of the skin," in *Proc. 3rd Augmented Hum. Int. Conf.*, 2012, pp. 1–4.

[4] K. Bark, J. Wheeler, P. Shull, J. Savall, and M. Cutkosky, "Rotational skin stretch feedback: A wearable haptic display for motion," *IEEE Trans. Haptics*, vol. 3, no. 3, pp. 166–176, Jul.–Sep., 2010.

[5] L. Kuang, M. Aggravi, P. R. Giordano, and C. Pacchierotti, "Wearable cutaneous device for applying position/location haptic feedback in navigation applications," in *Proc. IEEE Haptics Symp.*, 2022, pp. 1–6.

[6] N. A. Caswell, R. T. Yardley, M. N. Montandon, and W. R. Provancher, "Design of a forearm-mounted directional skin stretch device," in *Proc. IEEE Haptics Symp.*, 2012, pp. 365–370.

[7] L. Meli, I. Hussain, M. Aurilio, M. Malvezzi, M. K. O'Malley, and D. Prattichizzo, "The hBracelet: A wearable haptic device for the distributed mechanotactile stimulation of the upper limb," *IEEE Robot. Automat. Lett.*, vol. 3, no. 3, pp. 2198–2205, Jul. 2018.

[8] M. Sarac, T. M. Huh, H. Choi, M. R. Cutkosky, M. D. Luca, and A. M. Okamura, "Perceived intensities of normal and shear skin stimuli using a wearable haptic bracelet," *IEEE Robot. Automat. Lett.*, vol. 7, no. 3, pp. 6099–6106, Jul. 2022.

[9] H. Culbertson, S. Schorr, and A. M. Okamura, "Haptics: The present and future of artificial touch sensations," *Annu. Rev. Control Robot. Auton. Syst.*, vol. 1, pp. 385–409, 2018.

[10] K. O. Johnson, "The roles and functions of cutaneous mechanoreceptors," *Curr. Opin. Neurobiol.*, vol. 11, no. 4, pp. 455–461, 2001.

[11] F. McGlone, J. Wessberg, and H. Olausson, "Discriminative and affective touch: Sensing and feeling," *Neuron*, vol. 82, no. 4, pp. 737–755, 2014.

[12] G. Corniani and H. P. Saal, "Tactile innervation densities across the whole body," *J. Neuriophysiol.*, vol. 124, no. 4, pp. 1229–1240, 2020.

[13] M. Raitor, J. M. Walker, A. M. Okamura, and H. Culbertson, "WRAP: Wearable, restricted-aperture pneumatics for haptic guidance," in *Proc. IEEE Int. Conf. Robot. Automat.*, 2017, pp. 427–432.

[14] E. Pezent, A. Macklin, J. M. Yau, N. Colonnese, and M. K. O'Malley, "Multisensory pseudo-haptics for rendering manual interactions with virtual objects," *Adv. Intell. Syst.*, vol. 5, 2023, Art. no. 2200303.

[15] A. Adilkhanov, M. Rubagotti, and Z. Kappassov, "Haptic devices: Wearability-based taxonomy and literature review," *IEEE Access*, vol. 10, pp. 91923–91947, 2022.

[16] S. Kanjanapas, C. M. Nunez, S. R. Williams, A. M. Okamura, and M. Luo, "Design and analysis of pneumatic 2-DoF soft haptic devices for shear display," *IEEE Robot. Automat. Lett.*, vol. 4, no. 2, pp. 1365–1371, Apr. 2019.

[17] E. Battaglia, J. P. Clark, M. Bianchi, M. G. Catalano, A. Bicchi, and M. K. O'Malley, "Skin stretch haptic feedback to convey closure information in anthropomorphic, under-actuated upper limb soft prostheses," *IEEE Trans. Haptics*, vol. 12, no. 4, pp. 508–520, Oct.–Dec., 2019.

[18] H. Bai, S. Li, and R. F. Shepherd, "Elastomeric haptic devices for virtual and augmented reality," *Adv. Funct. Mater.*, vol. 31, no. 39, 2021, Art. no. 2009364.

[19] K. T. Yoshida, C. M. Nunez, S. R. Williams, A. M. Okamura, and M. Luo, "3-DoF wearable, pneumatic haptic device to deliver normal, shear, vibration, and torsion feedback," in *Proc. IEEE World Haptics Conf.*, 2019, pp. 97–102.

[20] A. Shtarbanov, "FlowIO development platform–The pneumatic "raspberry PI" for soft robotics," in *Proc. Conf. Hum. Factors Comput. Syst.*, 2021, Art. no. 479.

[21] E. H. Skorina et al., "Reverse pneumatic artificial muscles (rPAMs): Modeling, integration, and control," *PLoS One*, vol. 13, no. 10, 2018, Art. no. e0204637.

[22] K. Yoshida, X. Ren, L. Blumenschein, A. Okamura, and M. Luo, "AFREEs: Active fiber reinforced elastomeric enclosures," in *Proc. IEEE Int. Conf. Soft Robot.*, 2020, pp. 305–311.

[23] X. A. Wu et al., "Tactile sensing for gecko-inspired adhesion," in *Proc. IEEE/RSJ Int. Conf. Intell. Robots Syst.*, 2015, pp. 1501–1507.

[24] D. R. Deo, P. Rezaii, L. R. Hochberg, A. M. Okamura, K. V. Shenoy, and J. M. Henderson, "Effects of peripheral haptic feedback on intracortical brain-computer interface control and associated sensory responses in motor cortex," *IEEE Trans. Haptics*, vol. 14, no. 4, pp. 762–775, Oct.–Dec. 2021.

[25] K. Myles and M. S. Binseel, "The tactile modality: A review of tactile sensitivity and human tactile interfaces," U.S. Army Research Laboratory, Aberdeen Proving Ground, MD, USA, Tech. Rep. ARL-TR-4115, 2007.

[26] K. T. Yoshida et al., "Cognitive and physical activities impair perception of smartphone vibrations," *IEEE Trans. Haptics*, vol. 16, no. 4, pp. 672–679, Oct.–Dec. 2023.

[27] Z. A. Zook, J. J. Fleck, and M. K. O'Malley, "Effect of tactile masking on multi-sensory haptic perception," *IEEE Trans. Haptics*, vol. 15, no. 1, pp. 212–221, Jan.–Mar., 2022.

[28] S. Kuroki, "Anisotropic distortion in the perceived orientation of stimuli on the arm," *Sci. Rep.*, vol. 11, 2021, Art. no. 14602.

[29] T. Schlereth, W. Magerl, and R.-D. Treede, "Spatial discrimination thresholds for pain and touch in human hairy skin," *Pain*, vol. 92, no. 1, pp. 187–194, 2001.

[30] J. P. Clark and M. K. O'Malley, "Defining allowable stimulus ranges for position and force controlled cutaneous cues," *IEEE Trans. Haptics*, vol. 16, no. 3, pp. 353–364, Jul.–Sep. 2023.

[31] S. Y. Kim, J. P. Clark, P. Kortum, and M. K. O'Malley, "The influence of cue presentation velocity on skin stretch perception," in *Proc. IEEE World Haptics Conf.*, 2019, pp. 485–490.

[32] J. J. Fleck, Z. A. Zook, T. W. Tjandra, and M. K. O'Malley, "A cutaneous haptic cue characterization testbed," in *Proc. IEEE World Haptics Conf.*, 2019, pp. 319–324.